

Optimizing clinical dosing of combination broadly neutralizing antibodies for HIV prevention

Bryan T. Mayer [1], Allan C. deCamp [1], Yunda Huang [1,2,3], Joshua T. Schiffer [1,4,5], Raphael Gottardo [1], Peter B. Gilbert [1,6], Daniel B. Reeves* [1]

[1] Vaccine and Infectious Diseases Division, Fred Hutchinson Cancer Research Center, Seattle WA, USA

[2] Public Health Sciences Division, Fred Hutchinson Cancer Research Center, Seattle WA, USA

[3] Department of Global Health, University of Washington, Seattle, WA, USA.

[4] Department of Medicine, University of Washington, Seattle, WA, USA.

[5] Clinical Research Division, Fred Hutchinson Cancer Research Center, Seattle WA, USA

[6] Department of Biostatistics, University of Washington, Seattle, WA, USA.

*Corresponding author dreeves@fredhutch.org

Abstract. Broadly neutralizing antibodies are promising agents to prevent HIV infection and achieve HIV remission without antiretroviral therapy (ART). As learned from effective ART, HIV viral diversity necessitates combination antibody cocktails. Here, we demonstrate how to optimally choose the ratio within combinations based on the constraint of a total dose size. Optimization in terms of prevention efficacy outcome requires a model that synthesizes 1) antibody pharmacokinetics (PK), 2) a mapping between concentration and neutralization against a genetically diverse pathogen (e.g., distributions of viral IC50 or IC80), 3) a protection correlate to translate *in vitro* potency to clinical protection, and 4) an *in vivo* interaction model for how drugs work together. We find that there is not a general solution, and the optimal dose ratio likely will be different if antibodies cooperate versus if both products must be simultaneously present. Optimization requires trade-offs between potency and longevity; using an *in silico* case-study, we show a cocktail can outperform a bi-specific antibody (a single drug with 2 merged antibodies) with superior potency but worse longevity. In another practical case study, we perform a triple antibody optimization of VRC07, 3BNC117, and 10-1074 bNAb variants using empirical PK and a pre-clinical correlate of protection derived from animal challenge studies. Here, a 2:1:1 dose emphasizing VRC07 would optimally balance protection while achieving practical dosing and given conservative judgements about prior data. Our approach can be immediately applied to optimize the next generation of combination antibody prevention and cure studies.

Introduction

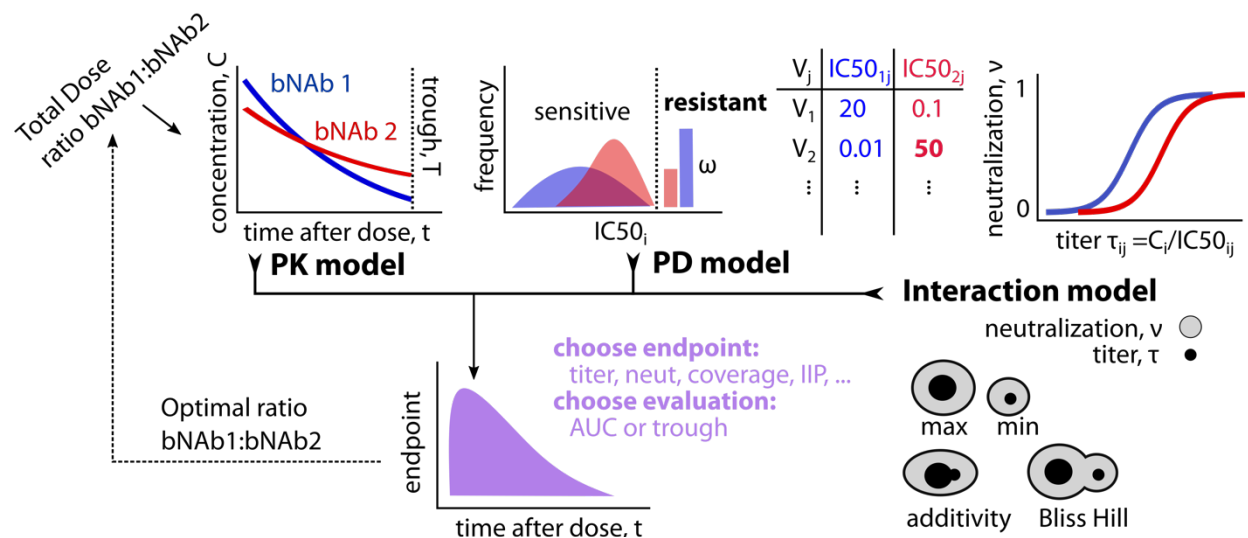
Broadly neutralizing antibodies (bNAbs) are powerful agents that may become crucial for next generation HIV prevention¹. Their utility is strengthened by their generally long half-lives compared to small molecule drugs, as well as the eventual promise of inducing bNAb production by vaccination^{2,3}.

The recent antibody mediated prevention (AMP) studies directly tested the hypothesis that the VRC01 bNAb could prevent HIV acquisition^{4,5}. While the study found no significant overall prevention efficacy, once HIV-1 Envelope pseudoviruses were made based on viral sequences from trial participants who acquired HIV-1 infection, it emerged that viruses acquired by placebo recipients were more sensitive to neutralization by VRC01 than viruses acquired by VRC01 recipients. The prevention efficacy against sensitive viruses (sensitive was defined as IC80 < 1 µg/ml) was estimated at 75.4% (95% confidence interval 45.5 to 88.9%). Less sensitive variants comparatively infected placebo and control recipients⁵. Indeed, the diversity of globally circulating strains⁶ remains beyond the breadth of any current bNAb. As with antiretroviral treatment (ART) and pre-exposure prophylaxis (PreP), combinations of products are likely needed⁷⁻⁹.

48 *In vitro* combination bNAb potency has been studied and modeled previously^{10,11}. Here, we extend these
 49 pharmacodynamic (PD) models to incorporate *in vivo* concentrations over time (pharmacokinetics, PK)
 50 with multiple bNAb administrations to establish a PKPD framework for clinical design focusing on how to
 51 ration the dose of each bNAb. A particularly important component of our modeling is that we allow bNAb
 52 concentrations to vary and distinguish *in vitro* and *in vivo* potency¹². As neutralization markers that best
 53 predict prevention efficacy (PE) are still under investigation, we consider flexible choices of the PKPD
 54 outcomes to be optimized, and also show that many outcomes are co-optimized. We apply our framework
 55 to 2 realistic *in silico* case studies. The first is a comparison of two antibodies against a bi-specific
 56 antibody^{13,14}, a synthesized combination of the two “parental” antibodies. We assume the bi-specific gains
 57 potency through the combination, but loses longevity, clearing with the faster of the two parental
 58 antibody half-lives. The second study models a three-drug combination of clinical candidate bNAb
 59 (VRC07-523-LS¹⁵, 10-1074 & 3BNC117¹⁶) and applies a protection correlate—protection predicted by
 60 neutralization titer—derived from non-human primate challenge studies¹⁷.

61 Our framework is designed to answer a crucial design consideration for these future studies: what is the
 62 optimal ratio of multiple antibodies to deliver in a single dose of a fixed size? We show the optimal ratio
 63 can depend on any and all inputs and assumptions -- precluding a one-size-fits-all solution. Instead, we
 64 provide a framework and a publicly available tool to determine the best dose plan given the specific
 65 antibodies, existing information about their interaction *in vivo*, and the PKPD outcome marker of interest
 66 for a proposed study. As more is known about each of these components, the model framework will rely
 67 on less uncertainty and become more predictive.

68 Results



69
 70 **Fig 1. PKPD model schematic for optimizing combination treatment against a genetically diverse**
 71 **pathogen.** The model incorporates: pharmacokinetics (PK), pharmacodynamics (PD), and interactions
 72 between antibodies. The PK describes antibody concentrations over time after administration. The PD
 73 model describes the distribution of neutralization potencies for each antibody against a variety of viral
 74 strains (quantified here by $IC50_{ij}$, the level of the i -th drug needed to achieve 50% neutralization of the j -th
 75 viral strain). We also allow some fraction ω of strains to be completely resistant. Then, from titer, or the
 76 ratio of concentration to $IC50$ of each antibody against a certain strain, we define neutralization using a
 77 logistic function, which defines the proportion (0-1 scale) of viruses that are neutralized. There are four
 78 functional PD interaction scenarios. The first two are heuristic taking either the worst (minimum) the best
 79 (maximum) titer or neutralization between two products. The other two are mechanistic combinations

80 described by independently combining titers (additivity) or neutralization (Bliss Hill). Then, depending on
81 the PKPD outcome measure of interest (for example titer, neutralization, coverage defined below) and
82 when that measure should be evaluated (throughout the study = AUC, at the low point = trough), we
83 identify the optimal ratio of the antibodies to be included in the initial dose.

84 We previously integrated pharmacokinetic (PK) and multi-strain pharmacodynamic (PD) models to
85 determine longitudinally varying potency of VRC01, a broadly neutralizing antibody (bNAb), to simulate
86 prevention trials and predict strain coverage^{18,19}. Because of HIV genetic diversity, it is essential to
87 consider the distribution of potencies against the diverse population of viral strains. We now extend this
88 framework to model multiple bNAbs, where integrating the combination PD models with PK adds several
89 layers of complexity (Fig 1).

90
91 **Pharmacokinetics (PK) for bNAb levels.** The first component of the PKPD framework is the PK, describing
92 concentrations of each antibody i over time, t : $C_i(\theta_i, t, d_i)$ where θ_i are the bNAb specific PK parameters
93 and d_i is the initial dose (PK model in Fig 1). Individual initial dosing for each bNAb is then constrained by
94 a total dose ($D = \sum_i d_i$). For simplicity, we assume a population-level fixed total dose and independent
95 models of PK for multiple bNAbs (denoted $C_i(t)$ from here on). The model could be extended to
96 implement individual-specific total dosing (e.g., bodyweight-adjusted) and joint, dependent models.

97
98 **Pharmacodynamics (PD) for bNAb potency.** Two pharmacodynamic (PD) quantities are often used to
99 discuss neutralization given concentration: 50% inhibitory dose or dilution neutralization titer (ID50 Titer)
100 and percent neutralization. Both quantities incorporate concentration and 50% inhibitory concentration
101 (IC50) measurements across a panel of viruses (PD model in Fig 1).

102 Experimental neutralization titer (ID50), $\tau_{ij}(t)$, is a common measurement arising from titrated
103 neutralization experiments. In practice, experimental ID50 represents a dilution factor applied to sera
104 containing antibodies that reduces *in vitro* neutralization to 50%. Titer, and the similarly derived ID80, are
105 important immunological endpoints that are proven correlates of protection^{4,17}. Experimental titer can be
106 theoretically predicted from the ratio of i -th drug concentration to j -th virus IC50 as

$$107 \tau_{ij}(t) = \frac{C_i(t)}{IC_{50ij}}, \quad \text{Eq 1}$$

108
109 a relationship that has been empirically confirmed for single bNAbs^{19,20}. As a potency measure, titer
110 expresses the fold-relationship between concentration and viral IC50 as a measure of ‘protection’ against
111 that virus.

112
113 Experimental *in vitro* neutralization for a single bNAb against a virus is also theoretically related
114 to the titer (Fig 1). Neutralization, on a 0-100% scale, has the mechanistic interpretation of the fraction of
115 blocked cellular infection events by the j -th virus, or “% neutralization”. Titer and neutralization, v , can
116 be related through the logistic Hill function (or median-effect equation) as follows

$$117 v_{ij}(t) = \{1 + \tau_{ij}(t)^{-h_{ij}}\}^{-1}. \quad \text{Eq 2}$$

118 Neutralization requires an additional parameter, the ‘Hill coefficient’ h_{ij} , that describes the steepness of
119 the neutralization curve. Through Eq 2, any generalized titer (e.g., ID80, ID99) can be predicted from the
120 ID50 titer and a given Hill slope, where the Hill slope can be estimated from IC50 and IC80 measurements
121 (see **Supplementary Information**). Using the CATNAP database²¹ of IC50 and IC80 neutralization estimates
122 for HIV virus/antibody combinations, we estimated the distribution of Hill slopes and generally found
123 values near 1 (See Methods and **Supplementary Figure 1**). Henceforth in our analysis, and consistent with
124 previous measurements¹⁸, we set $h_{ij} = 1$ and it is dropped from equations. Under this assumption, the

125 IC80 is theoretically predicted to be 4-fold higher than the IC50, and, subsequently, the ID80 is predicted
 126 to be 4-fold lower than the ID50 for single bNAb and virus combinations (see **Supplementary Information**
 127 for more details).

128
 129 **bNAb interaction models.** For bNAb combinations, we considered 4 PD interaction models. The first, Bliss-
 130 Hill independence (BH), is the best-case multiplicative interaction where bNAbs cover missing breadth of
 131 one another and co-neutralize strains, i.e., virions must escape independent binding events from each
 132 antibody. BH is encouragingly observed from *in vitro* studies^{10,22}. We also consider weaker cooperation
 133 with the additivity interaction model, where antibody effects are combined via mass action¹⁰; i.e., the
 134 total titer is sum of individual titers. Finally, maximum and minimum models assume that the more or less
 135 potent antibody for each strain operates as a single product. The maximum interaction potentially
 136 represents a scenario where only the most potent bNAb neutralizes a given virus; however, outcome
 137 deviations between the maximum and the BH or additivity model also highlight where interactions
 138 improve neutralization due to combined coverage. On the other hand, the minimum model is
 139 mechanistically unrealistic but provides a boundary for the worst-case scenario where the combination
 140 regimen is only as strong as its weakest link, specifically penalizing poor combined coverage of viruses.

141 The interaction models are mathematically summarized in **Table 1** and all derivations of
 142 combinations titers are included in the **Supplementary Information**. We extend interactions to include
 143 synergy in the bi-specific antibody case study, but do not consider antagonism among clinically viable
 144 bNAb combinations here.

145 **Table 1.** Summary of equations for PD interaction models relating bNAb (*i*) to virus (*j*). Formula for Bliss-
 146 Hill ID50 illustrated for 2-bNAb combinations only.

PD Outcome	Bliss Hill (BH)	Additivity	Maximum	Minimum
Titer (ID50) $\tau_{ij}(t)$, Eq 1	$\frac{2\tau_{1j}\tau_{2j}}{-(\tau_{1j} + \tau_{2j}) + \sqrt{(\tau_{1j} + \tau_{2j})^2 + 4\tau_{1j}\tau_{2j}}}$	$\sum_i \tau_{ij}(t)$	$\max_i[\tau_{ij}(t)]$	$\min_i[\tau_{ij}(t)]$
Neutralization $v_{ij}(t)$, Eq 2	$1 - \prod_i [1 - v_{ij}(t)]$	$1 - \left[1 + \sum_i \tau_{ij}(t)\right]^{-1}$	$\max_i[v_{ij}(t)]$	$\min_i[v_{ij}(t)]$

147
 148 Other options exist to quantify antibody potency, including instantaneous inhibitory potential (IIP²³), the
 149 log-fold reduction in virus infectivity at a given concentration, which linearizes high neutralization on the
 150 log-scale (e.g., 99% neutralization → IIP of 2, 99.9% → 3) in the important range for ART efficacy²³.

151
 152
$$\text{IIP}_{ij}(t) = -\log_{10}[1 - v_{ij}(t)] = \log_{10}[1 + \tau_{ij}(t)].$$
 Eq 3

153
 154 A generalized version of IIP when $h_{ij} \neq 1$ is described in the **Supplementary Information**.

155 Alternatively, the potency of an antibody combination can be quantified by its “viral coverage”:
 156 what fraction of viral strains are above a specified threshold value. Fundamentally, the neutralization
 157 measurement is dichotomized for a given bNAb/virus combination, i.e., the virus is neutralized or not
 158 based on some measurement threshold. For example, for *n* strains and a neutralization threshold v^* , we
 159 define the neutralization coverage fraction $f(t, v^*) = \frac{1}{n} \sum_{j=1}^n \mathcal{J}(v_{ij}(t) > v^*)$ where \mathcal{J} is the indicator
 160 function equal to 1 if the inequality holds and 0 otherwise.

161

162 **Mathematical model for optimizing antibody combination doses.** Finally, we summarize these
163 measurements of potency over time, which we collectively term PKPD outcomes. We consider PKPD
164 outcomes at trough (pre-specified final time) or throughout time (area under the curve, AUC) (**Fig 1**).

165 In practice, for a specified antibody combination, we obtain their PK parameters and the best
166 estimate of their distribution of IC50s to a relevant panel of circulating viruses. We can then choose an
167 interaction model and specify an outcome that we want to optimize. From this we uniquely determine
168 the optimal ratio of the antibodies. Potential combinations of bNAbs—varying by their input PK and PD
169 profiles—can then also be evaluated and compared via mathematical PKPD simulations at the optimal
170 dosing ratios, which may be combination-dependent, as illustrated in the *in silico* studies below.

171 **Global sensitivity analysis.** Across a range of theoretical 2-bNAb combination studies, we performed a
172 global sensitivity analysis varying all input PKPD model parameters (**Fig 1**) to assess correlation between
173 all PKPD outcomes and optimized dosing ratios (see **Methods**). Briefly, we varied one-compartment
174 exponential PK models for each antibody summarized by their half-life hl_i . One bNAb was simulated to
175 always have equivalent or better half-life than the other to avoid redundancy. We chose a log-normal
176 distribution for IC50s for each bNAb parameterized by its mean μ_i and standard deviation σ_i on the log10
177 scale, also allowing for a fraction ω_i that are completely resistant (infinite IC50). We also varied the ratio
178 of doses r and the total dose D . The ranges explored for each sensitivity analysis parameter are collected
179 in **Table 2**.

180

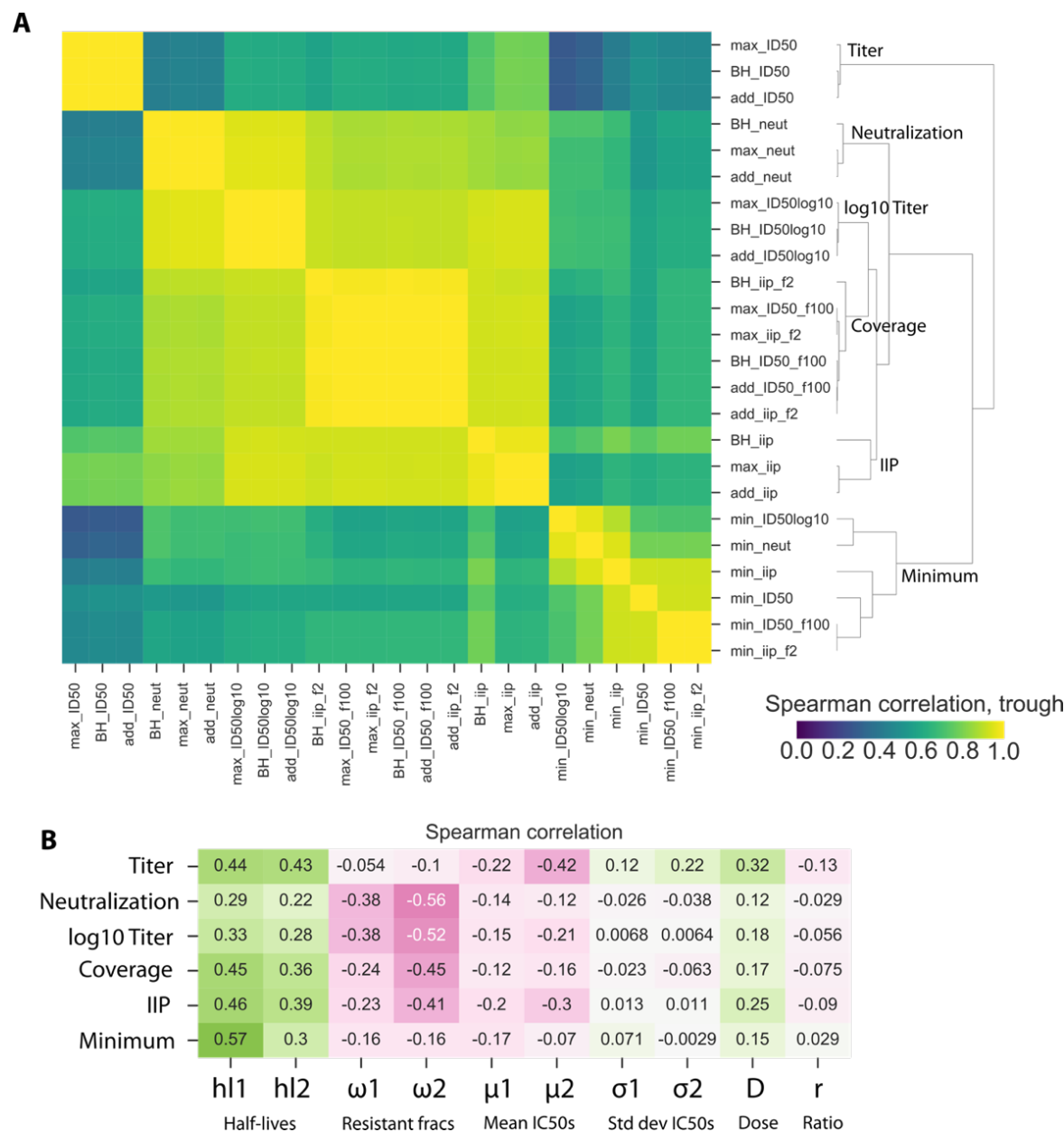
181 **Table 2.** Parameter settings for PKPD sensitivity analysis for combining 2 bNAbs.

Parameter	Sensitivity analysis values
Initial dose (mg)	{150, 300, 600, 1200, 2400}
Half-life (days)	{7, 28, 42, 84}
Total simulated viruses	500
% viral resistance	{67, 33, 0}
Mean log10 IC50 ($\mu\text{g}/\text{mL}$)	{-3, -2, -1}
SD log10 IC50 ($\mu\text{g}/\text{mL}$)	{0.25, 0.5, 1}

182

183 **Publicly available tool for ratio optimization.** Any individual simulation from the results can be generated
184 using the following R shiny app: <https://bnabpkpd.fredhutch.org>.

185 **PKPD outcomes cluster into categories.** Using global sensitivity analysis output, we calculated Spearman
186 correlations among all endpoints at trough (**Fig 2A**). By hierarchical clustering, we determined six main
187 categories of outcomes (**Fig 2A**): All models with the minimum interaction (i.e., worst-case bNAb
188 penalizing lack of combination viral coverage) and raw titer (ID50) endpoints for the non-minimum
189 interaction were quite distinct. The remaining outcomes were correlated but further categorized as
190 neutralization, \log_{10} -transformed titer, coverage metrics (% of viruses neutralized > 99%), and IIP. Results
191 were similar for AUC and trough, see **Supplementary Fig 2**, which indicates for a simple monotonic PK
192 curve, the final value is representative of the entire time-course.



193

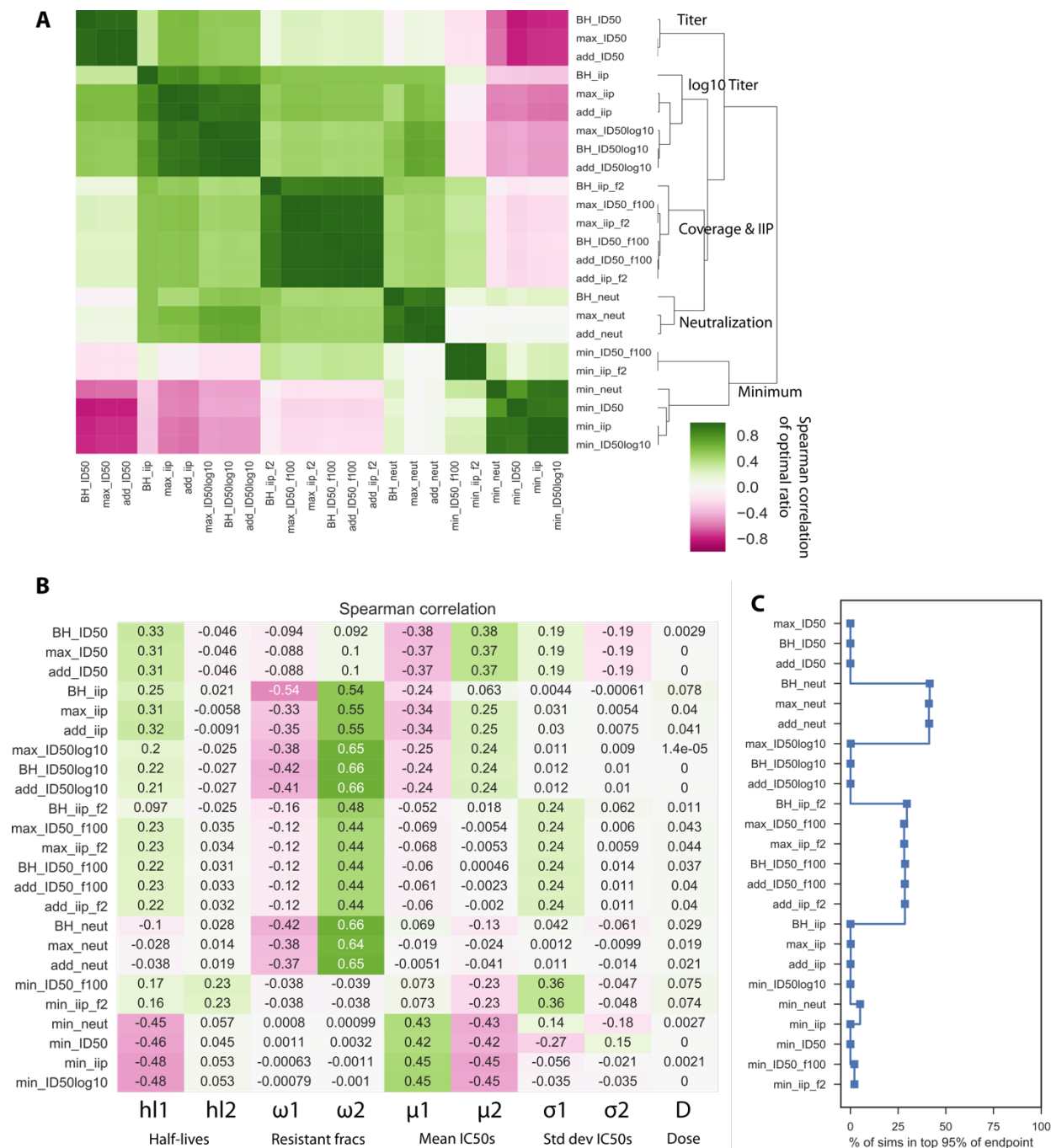
194 **Fig 2. Correlations among PKPD outcomes and between model parameters and outcomes.** We
 195 performed a global sensitivity analysis to simulate a two-drug combination therapy against a genetically
 196 diverse pathogen where the drug 1 had equivalent or worse half-life than drug 2. We simulated 24
 197 outcomes at trough (results for AUC are similar), including ID50, log10 ID50, neutralization, instantaneous
 198 inhibitory potential (IIP), as well as the coverage fraction of pathogen strains having ID50>100 and IIP>2.
 199 A) Many of these outcomes are strongly correlated (yellow in heatmap). Moreover, these 24 outcomes
 200 cluster into approximately 6 distinct categories: see labels along dendrogram. Of the interaction models,
 201 only the minimum interaction separated into its own category while the others clustered together within
 202 a given outcome. B) Overall, we varied 10 model parameters (Table 2). By correlating (Spearman, green~1,
 203 pink~-1) to the 6 categories from panel A against all model parameters, we found that the categories were
 204 similarly sensitive to PK, while titer and minimum categories were less sensitive to resistance fractions. The
 205 ratio does not strongly predict any outcomes when all other parameters are varied, highlighting that there
 206 is no general solution to optimizing the ratio and it must be adjusted on a case-by-case basis.

207 **Correlations among PKPD outcomes and antibody features.** We next explored the associations between
208 a representative member of each outcome category and model parameters (**Fig 2B**). All categories were
209 sensitive to PK (half-life), and generally more to the half-life of the shorter-lived bNAb (hl2). Increased
210 resistance negatively correlated with the outcomes, particularly with neutralization, \log_{10} -transformed
211 titer, coverage metrics, and IIP. Additionally, a stronger negative correlation was found with the resistant
212 fraction for the bNAb with longer half-life – this pattern was weaker for mean IC50. Total dose correlated
213 positively with all outcomes but was generally less influential than other model parameters. The ratio of
214 antibodies did not strongly predict any outcome after accounting for variation in all other parameters,
215 highlighting that there was no generally optimal ratio; optimization is determined on a case-by-case basis
216 based on many antibody features.

217
218 **Sensitivity of the optimal ratio for each outcome.** Next, for each parameter set, we determined the
219 optimal ratio r for each outcome. **Fig 3A** shows an analogous clustering analysis to **Fig 2** but with
220 correlations of the *optimal ratio* of each outcome across the inputs. Importantly, the same categories
221 emerged such that correlations among all outcomes agreed generally with correlations among optimal
222 ratios. In particular, the optimal ratio for minimum not only appears distinct from the other categories
223 but is often negatively correlated to the others. This suggests that optimizing for minimum interaction
224 (i.e., maintaining consistent combination coverage) may require a very different ratio. For the other
225 interactions, once an outcome is selected, the optimal ratios generally agree among maximum, additive,
226 and Bliss-Hill interaction models.

227 **Fig 3B** shows correlations among optimal ratios for each outcome and model parameters. Here
228 directionality of correlation has additional meaning: positive and negative correlations imply less or more
229 of the antibody with worse half-life, respectively. The sensitivity to PK and PD (resistance and mean IC50)
230 followed the same pattern as in **Fig 2A**: all the outcomes showed some sensitivity to PK, titer and minimum
231 interaction outcomes were sensitive to mean IC50, and the remaining were sensitive to resistance
232 fractions. For ratio optimization, the PK sensitivity was specifically driven by the half-life of the shorter-
233 lived bNAb.

234 We next sought to understand what is gained by using the optimal ratio as opposed to a more
235 practical solution near the optimum. Therefore, we measured how many parameter combinations
236 admitted an outcome within 95% of the outcome value achieved by the optimal ratio (**Fig 3C**). That is, if
237 most simulations were within 95% of the optimum, it means the optimum is not substantially better.
238 Indeed, for the parameter ranges we considered, some outcomes were not particularly sensitive to the
239 choice of the optimal ratio such that other practical considerations could be promoted in a trial design.
240 However, some outcomes were much more strongly affected by optimization (with fewer than $1/10^4$ runs
241 being in the 95% optimal scenario) including IIP. So, although there are cases of insensitive systems (e.g.,
242 two poor products, two highly effective products), this reinforces that optimization should be case-
243 specific.



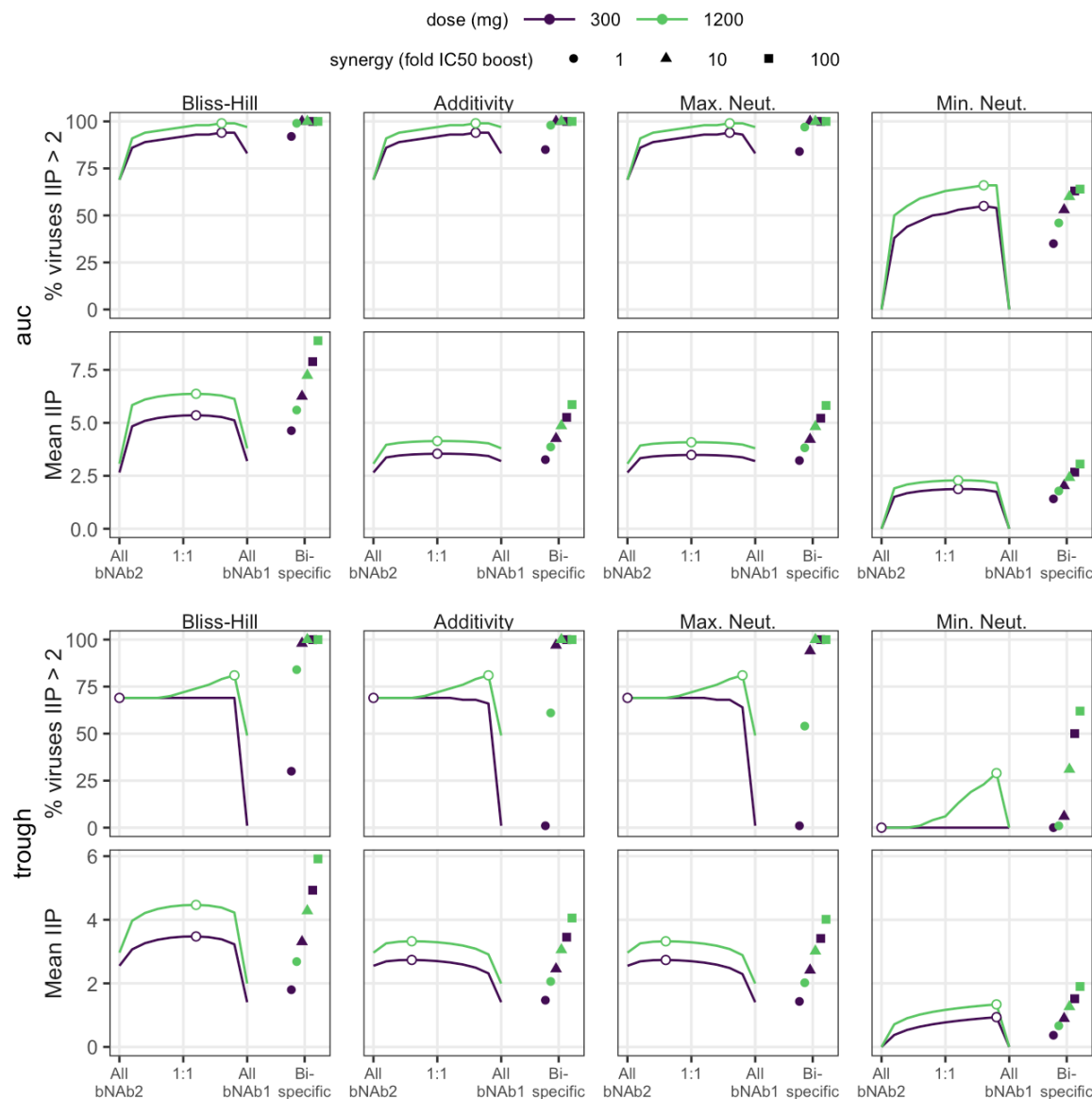
244
 245 **Fig 3. Sensitivity of the optimal ratio to PKPD outcome choices and antibody features.** From the global
 246 sensitivity analysis, we calculated the optimal ratio for each parameter set and each outcome. (A) We
 247 repeated the clustering analysis to determine how the optimal ratio clusters by outcome. In this setting
 248 coverage and IIP cluster together leading to 5 (rather than 6) categories, but the others remain the same
 249 from the prior analysis in Fig 2. B) Certain variables drive optimization for different outcomes. For example,
 250 the mean IC50 are most influential on optimizing ratios using minimum neutralization and titer outcomes,
 251 while the fraction resistant is most influential for the remaining outcomes. C) Across all simulations, we
 252 quantified the sensitivity of the optimal ratio of each outcome by calculating the fraction of parameter
 253 sets in which the outcome was within 95% of its optimal value. For the parameter ranges considered, some

254 *of these outcomes were not enhanced greatly by perfect optimization, but outcomes clustered in the*
255 *correlation showed similar sensitivity and some outcomes were particularly sensitive.*

256
257 **Dual parental antibodies outperformed bispecific product without synergy enhancement.** Bi-specific
258 antibodies, synthesized combinations of two antibodies into one product, appear *in vitro* to exhibit
259 superior neutralization compared to their parental components^{13,14}. However, these experiments are not
260 inclusive of *in vivo* pharmacokinetics. Bi-specific antibody clearance may be determined based on the
261 clearance kinetics of either parental component. If clearance characteristics are comparable to the slower
262 of the two parental antibodies, then the bi-specific combination is clearly advantageous. Because bi-
263 specific PK is not well studied, we tested the non-trivial scenario in which a bi-specific inherits the worse
264 (faster) parental half-life. We investigated a realistic design administering 300 or 1200 mg of antibodies
265 and 3-month administration window. We assumed one parental antibody had a 3-month half-life
266 equivalent to the trough time but with worse PD than a superiorly potent bNAb. However, the more
267 potent bNAb was given a poorer half-life of 1 week (i.e., equivalent to 1/12 of trough window). We
268 evaluated the theoretical study efficacies using the following PKPD outcomes: a continuous outcome
269 (mean IIP) and a coverage outcome (% viruses IIP>2).

270 Compared to the combination therapy, the superior potency of the bi-specific antibody is not
271 necessarily sufficient to account for a poor PK profile. Across doses and interaction models, we
272 consistently found that the optimal combination therapy was more efficacious than the bi-specific for
273 both AUC and trough (**Fig 4**). At trough, where half-life had higher influence, the parental with better half-
274 life but worse PD alone outperforms the bi-specific particularly at lower doses.

275 Given this finding, we tested how much additional synergy (as a factor multiplying the bi-specific
276 potency through reduced IC50, see **Methods**) could rescue the bi-specific performance and make it
277 comparable to the parental combination. Synergy has been observed for bi-specifics because binding of
278 one antibody arm can facilitate the second to bind²⁴. Using synergy models, the bi-specific outperformed
279 the optimized combined administration when the synergy factor exceeded 10-fold under common
280 interaction models (**Fig 4**).



281
 282 **Fig 4. Optimizing 2 bNAb combination therapy in comparison to bi-specific therapy with the same**
 283 **bNAbs.** Combination antibody results for AUC (top) and trough (bottom) suggest that trough is slightly
 284 more sensitive to ratio (see curvature of outcome surface and change from optimal ratio denoted by open
 285 dot). In general, a single bi-specific bNAb will perform worse than combination therapy if it has the best
 286 neutralization potential of both parental lineages under a common interaction model but inherits the
 287 faster clearance kinetics. However, if synergetic binding occurs, enhancing the bi-specific potency by 10-
 288 fold (see **Methods**), it is similar or outperforms the optimal combination for all outcomes and doses. “All
 289 bNAb1” and “All bNAb2” on the x-axis correspond to 100% dosing of the second bNAb product.

290 **Incorporating empirical protection correlates in clinical design.** To perform a realistic optimization of a
 291 clinical trial, we consider deviations from *in vitro* potency that may be relevant for *in vivo* protection. For
 292 example, non-human primate HIV challenge studies suggest that a bNAb titer of approximately 100
 293 achieved 50% protection: i.e., serum antibody concentrations need to be 100-fold higher than *in vitro* IC50
 294 to elicit 50% protection *in vivo*¹⁷. We define the fold-increase as a “potency reduction factor”¹⁸, ρ , and

295 henceforth translate *in vitro* potency to *in vivo* protection by scaling the titer input. We have *in vivo*
296 neutralization and IIP then,

$$297 \quad v^{invivo}(t) = \left\{ 1 + [\tau_{ij}^{invitro}(t)/\rho]^{-1} \right\}^{-1}, \quad \text{Eq 4}$$

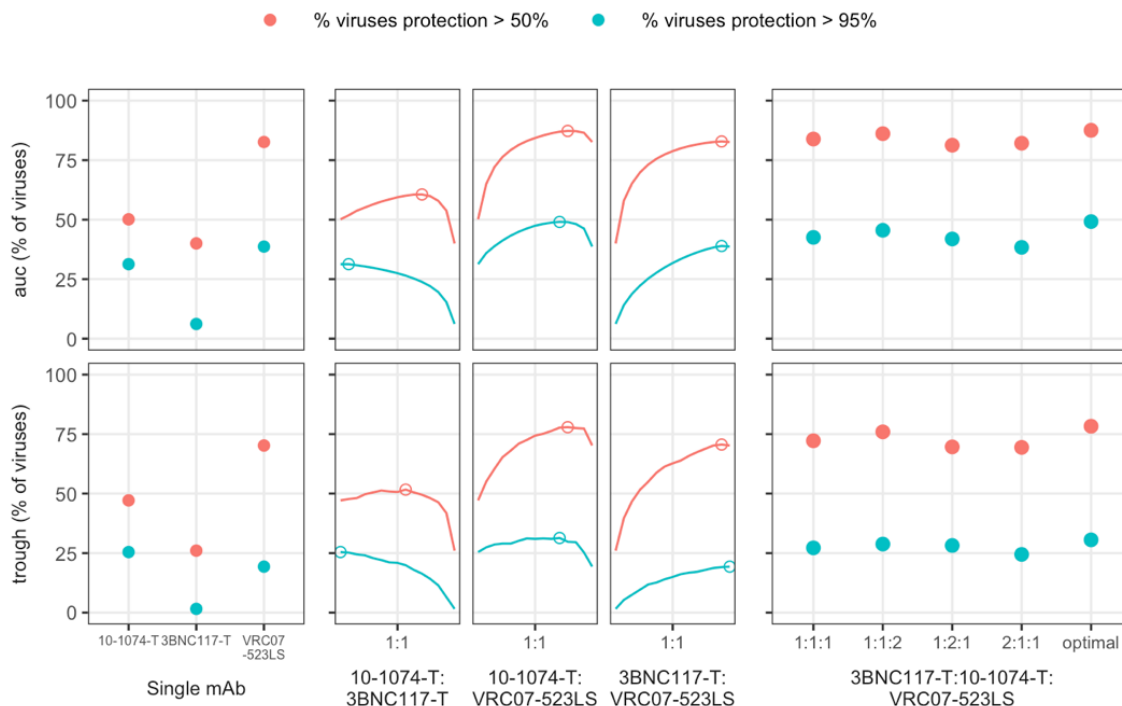
$$298 \quad IIP_{ij}^{invivo}(t) = \log_{10}[1 + \tau_{ij}^{invitro}(t)/\rho]. \quad \text{Eq 5}$$

299
300 such that no change from *in vitro* measured titer occurs when $\rho = 1$ and a potency reduction of 100-fold
301 means $\rho = 100$. Mechanistically, this formulation suggests that the overestimated protection *in vivo* is
302 due to either (or both) underestimation of the potency due to some biological factors (e.g. coagulation or
303 anti-antibody elements) or overestimation of bNAb concentration at the site of exposure.

304 The reduction factor can be derived from assessing actual protection at the given experimental
305 titers, either through NHP challenge or using protection efficacy (PE) estimated from clinical study.
306 Alternatively, if multiple protection estimates for varying titers, the titer vs. protection dose-response
307 relationships can also be structurally varied; for example, we employed a 5-parameter logistic model on
308 the NHP protection data for the following case study (see **Methods**).

309 For combination bNAbs, the experimental titer will represent neutralization in sera with a
310 combined concentration of antibody. Whether a potency reduction factor is applied to the combination
311 titer or to the individual titers prior to the interaction is specifically consequential for the Bliss-Hill
312 interaction model, but not the other interaction models. Briefly, applying the factor to the Bliss-Hill
313 combination titer model may be overly conservative, underestimating the protection because
314 experimental titer does not uniquely predict Bliss-Hill neutralization (**Supplementary Figure 3**; see
315 **Supplementary Information** for further discussion). We suggest applying the potency factor or protection
316 model to each bNAb individually, calculating their individual protection estimate, then applying the Bliss-
317 Hill interaction model (i.e., at the event-level) as described in the following case study.

318
319 **Using empirical protection correlates in a 3-bNAb optimization.** We gathered several independent data
320 sets to model a 12-week trial with a 600 mg subcutaneous dose of 3 state-of-the-art broadly neutralizing
321 antibodies (3BNC117-T, 10-1074-T, VRC07-523-LS; -T denotes theoretical variant with extended half-life).
322 For this example, we used an empirical protection estimates based on titer from the Pegu *et al.* NHP meta-
323 analysis¹⁷ with the primary PKPD outcome of viral coverage at 50% and 95% protection thresholds. For
324 more details on the input PK and PD for these analytes, see **Methods** and **Supplementary Figure 4**. In this
325 illustrative example, we do not consider clade-specific profiles nor account for interference potentially
326 due to 3BNC117 and VRC07-523-LS targeting the same epitope (CD4-bs). Next, we tested all double and
327 triple combinations varying the dosing ratios. In a clinical setting, it is unlikely that complicated dosing
328 ratios would be of practical consideration (e.g., 98:13:3). Thus, for the 3-bNAb combination, we
329 considered simple ratio designs: an even dose split (denoted 1:1:1) or any 50%:25%:25% combination
330 (denoted 2:1:1 or similar). We compared this to the theoretical optimum to ensure they were reasonably
331 close to the optimal design.



332
 333 **Fig 5. Additional enhancement after optimization of 3-drug therapy.** Using 3 well known anti-HIV broadly
 334 neutralizing antibodies, we performed an analysis comparing the percent of viruses at more than 50% and
 335 95% neutralization level for the bNAbs individually, in 1:1 combination, and in triplicate as 1:1:1, 1:1:2,
 336 1:2:1, 2:1:1, and the optimal combination (see **Table S2**). Enhancement over the best single bNAbs (VRC07-
 337 523-LS) is generated through combinations when evaluating the percent of the viruses neutralized at a
 338 95% level. However, triple drug therapy does not meaningfully enhance over optimized 2-drug therapy
 339 levels, even when completely optimized. Indeed, a 1:1:1 3 drug therapy is outperformed by the optimized
 340 2-drug therapy, highlighting the need to carefully perform case-studies for any optimization scenario.
 341 Overall, all triple drug combinations predicted a protection level above 95% for roughly 25% of viruses at
 342 trough. Likewise, protection levels were above 50% for roughly 80% of viruses over the study (AUC). It
 343 was clear that VRC07-523LS was the best single antibody, and the optimal dosing ratio generally contained
 344 >60% of VRC07-523-LS (see **Table S2**). Subsequently, the triple combination with 1:1:2 level of VRC07-
 345 523LS was not much worse than optimal. Moreover, the optimal 2-drug combination without 3BNC117-T
 346 was nearly as effective as the optimal 3 drug therapy (which dosed at <10% of 3BNC117-T) potentially due
 347 to general lower potency of 3BNC117 or the overlap in epitope targeting with VRC07-523-LS resulting in
 348 redundant viral coverage in the database. Still, given our necessarily incomplete data on circulating
 349 strains, we would suggest using this 3-drug therapy at a 1:1:2 design to balance simplicity and protection
 350 for this example.

351 Discussion

352 Combination administration of broadly neutralizing antibodies is likely to form a key component of future
 353 studies of HIV prevention^{1,4,14,25}. While antibody neutralization is essential, accurate balancing of antibody
 354 dosing requires modeling both neutralization and concentration levels over time. Our approach here
 355 addresses this critical unmet need.

356 Our analysis highlights that several types of data for each antibody in a combination modality must all be
357 considered to optimize dosing rationally. These include 1) the input potency data relating each bNAb to
358 existing *in vitro* assays that test drug potency (i.e., IC50); 2) a translation to an *in vivo* protection metric
359 using a correlate derived from NHP meta-analysis; and 3) an understanding of drug interactions. The
360 second step is crucial because *in vitro* IC50 measurements could underestimate *in vivo* efficacy^{18,26}. While
361 we illustrate use of a NHP correlate, human correlates may soon be derived from the AMP trials. The best
362 correlate will likely need to be translational using readily available *in vitro* neutralization data for
363 predictions^{14,22}, which may be calculated using pseudoviruses (e.g., CATNAP database²¹) or breakthrough
364 viruses in human infections²⁷.

365 Here, we depict how to implement a titer protection correlate into clinical design for combinations. As
366 illustrated in our practical case study design using the NHP challenge correlate, we derive a dose-response
367 relationship for titer and protection from the NHP challenge studies, and then assess combinations using
368 this empirical protection as the PKPD outcome via viral coverage. We also highlight that the protection
369 estimates derived from single bNAb studies need to be carefully translated into combination bNAb target
370 outcomes. Specifically for the Bliss-Hill interaction, a combination sera titer may correspond to different
371 protection estimates depending on the underlying individual concentrations of each bNAb. We suggest
372 determining antibody-level protection first then applying the BH interaction. This approach is also
373 amenable if different potency reduction factors or dose-response protection relationships are bNAb-
374 specific depending on target site.

375 Because there remains uncertainty regarding the optimal PKPD protection endpoints for bNAb
376 combinations, our sensitivity analysis illustrates several main categories with similar properties.
377 Moreover, we show certain features of antibodies (long half-lives, broad coverage, etc.) are particularly
378 predictive of success, raising the possibility of using these results to inform endpoint selection based on
379 coarse knowledge of circulating strains. While PK heterogeneity will affect endpoints and should be
380 considered for optimizing trial design, the endpoints we tested exhibited much more sensitivity to the PD
381 profile of the product. The optimal ratio of a two-drug therapy was shown to be strongly sensitivity to
382 specifics of the combined antibody features. Thus, in combination with additional demographic
383 considerations and population risk, we advocate for specific optimization for any trial rather than relying
384 on general rules. Additionally, certain endpoints are more sensitive to optimal dosing than others, which
385 can be considered in endpoint selection, or alternatively, if an endpoint is preferred which is not
386 particularly sensitive, practical considerations about dosing could be prioritized over precise dose
387 optimization as illustrated by our 3-bNAb combination example.

388 In our sensitivity analysis, we also find that PKPD outcome levels and optimal ratio are well correlated
389 between the maximum, additivity, and BH interaction. This suggests that the design of the trial is not
390 particularly sensitive to selecting the correct interaction model among these choices; however, the correct
391 choice may still improve the accuracy of the predicted PKPD outcome. On the other hand, the minimum
392 interaction formed a unique cluster of simulated endpoints and optimized compared to others. While the
393 minimum interaction may be unrealistic, it explicitly penalizes designs that lack effective combination
394 coverage. In practice, a trial optimization may evaluate both a minimum and Bliss-Hill interaction
395 endpoints, allowing the minimum interaction to represent a worst-case scenario where there is no
396 protection against viruses without sensitivity to at least two bNABs.

397 Although most of our analysis concerns prevention studies, this framework is applicable to curative
398 studies attempting to use bNABs to prevent viral rebound after stopping ART^{28,29}. The challenge in this
399 setting is within-host diversity in the reservoir. Blocking a single founder during a transmission event
400 appears easier than blocking repeated reactivations of diverse viral populations. Several studies have
401 illustrated bNABs can delay viral rebound²⁸⁻³⁰. However, levels required to prevent rebound remain hard

402 to predict. In a cohort of 18 individuals receiving VRC01 infusion and ART cessation rebound occurred
403 when plasma VRC01 levels were well above *in vitro* IC50s²⁹.

404 Our analysis shows potential limitations around bi-specifics once PK is considered. Specifically, if the
405 synthesized product clears faster, performance can be worse than an optimized combination therapy of
406 the two parent products. The prevention benefits from bi-specific products thus rely on beneficial co-
407 binding represented through some synergy, but these benefits may trade off with poorer half-life.
408 Without synergy, bi-specifics are effectively a 2-fold concentration bonus, but neutralization is relatively
409 insensitive on this scale, requiring input changes on the log-scale to either IC50s or concentrations. Of
410 note, a powerful synergistic effect may allow these products to be potent at unmeasurable concentrations
411 (i.e., below a typical limit of detection), which may not be tenable for study and practical use in a clinical
412 setting. On the other hand, bi-specifics may be clinically preferable as they are a single product, and if the
413 PK is at least half the dosing interval (or trough time), then our analysis suggests they theoretically perform
414 comparably or better than combinations without consideration of synergy.

415 The three-drug optimization exercise illustrates that one potent antibody can determine the ability of
416 combinations. Indeed, in this specific example, a two-drug therapy would have been nearly as good.
417 However, in considering that viral panels are necessarily incomplete, we would err on the side of
418 inclusivity to both widen breadth and account for uncertainty about escape mechanisms. In this example,
419 adding the third and optimizing the triple-drug ratio is always beneficial to the two-drug combination,
420 albeit minorly.

421 Going forward, our recommendation for designing therapeutic combinations for prevention or treatment
422 of diverse pathogens is several fold: 1) choose outcomes based on expert opinions and given
423 disagreements, assess whether these qualitative decisions are actually quantitatively in agreement; 2)
424 consider multiple, distinct outcomes to evaluate a range of potential results; 3) optimize drug ratios for
425 the specifics of component features; and 4) include subdominant levels of weaker antibodies to
426 potentially cover holes in coverage not observable from incomplete preliminary data.

427 **Methods**

428 **Code and data.** All analysis were performed in R and Python. Simulations, data processing, and
429 visualizations performed using R used the *tidyverse* package suite³¹. Sensitivity and cluster analysis of
430 simulation results with subsequent visualizations were performed using the *seaborn* library in Python. All
431 code will be available on GitHub.

432 **Estimation of Hill slope using CATNAP data.** The Hill slope in the 2-parameter logistic Hill function (Eq 2)
433 can be estimated from the IC50 and IC80 measurements (formula derived the **Supplementary**
434 **Information**). We estimated the distribution of the neutralization Hill slope by performing this calculation
435 across virus/antibody combinations available in the LANL CATNAP database²¹. To accommodate assay
436 quantification limits that potentially vary across experimental study, we limited the analysis datasets to
437 IC50 and IC80 values between 0.01 and 20 ug/mL, comprising 20,236 total combinations. Additionally, we
438 grouped calculations within quartiles of input IC50 to assess whether Hill slopes vary by underlying viral
439 sensitivity or measurement error that varies with the scale of IC50.

440 **Global sensitivity analysis.** We performed ~10,000 simulations over all combinations of parameters in
441 Table 2 and calculated all PKPD outcomes. We chose a one-compartment exponential PK model with
442 trough time 84 days for each bNAb: $C_i(t) = C_i(0) \exp(-k_i t)$, and summarized the PK model with its half-
443 life $hl_i = \ln 2/k_i$. The PK model used a one compartment model with fixed volume of distribution (3 L)^{32,33}.
444 One bNAb was simulated to always have equivalent or better half-life than the other to avoid redundancy.
445 We chose a log-normal distribution for IC50s for each bNAb parameterized by its mean μ_i and standard

446 deviation σ_i on the \log_{10} scale, also allowing for a fraction ω_i that are completely resistant (infinite IC50).
447 We sampled 500 viruses per simulation. We then varied these parameters, along with the ratio of doses
448 r and the total dose D . Then, we determined the optimal ratio as the ratio that maximized each PKPD
449 outcome for all other parameter values across interaction models. To calculation IIP under Bliss-Hill,
450 neutralization calculated for each bNAb and used as input, not titer (see **Supplementary Information**).
451 Using the seaborn package in Python, we performed hierarchical clustering of Spearman correlations
452 among outcomes and between parameters and outcomes.

453
454 **Comparison of bi-specific to parental antibodies.** For the first parental bNAb, we chose a potent
455 neutralizer (mean IC50 of 10^{-3} with 0% viral resistance) but with poor PK: elimination half-life equivalent
456 to 1/12 of the administration period (i.e., 7-day half-life for an 84-day trough). For the second bNAb, we
457 chose a more modest neutralizing profile (mean IC50 of 10^{-2} with higher variance and 33% viral
458 resistance) but with excellent PK: elimination half-life equivalent to one administration period.
459 To model the bi-specific, we assumed the single molecule formulation means two parental products are
460 given at the identical dose. We also assumed the clearance PK was determined by the faster of the two
461 parental products. We additionally allowed for synergy, such that each antibody's potency is improved by
462 a factor α . This factor was assumed to be the same for all viral strains. Thus, following **Eq 3** and **Table 2**,
463 the bi-specific IIP against a single virus V_j can be calculated for max, min, and additivity models,
464 respectively

$$465 \text{IIP}_j = \log_{10} \left[1 + \alpha \min_i \tau_{ij} \right], \quad \text{Eq 6}$$

$$466 \text{IIP}_j = \log_{10} \left[1 + \alpha \max_i \tau_{ij} \right], \quad \text{Eq 7}$$

$$467 \text{IIP}_j = \log_{10} \left[1 + \alpha \sum_i \tau_{ij} \right]. \quad \text{Eq 8}$$

468
469 For Bliss-Hill interaction, the derivation from individual titers to a combination IIP is shown in the
470 **Supplementary Information (Eqs S27 & S29)** and then the bi-specific synergy was implemented as follows:
471

$$472 \text{IIP}_j = \sum_i \log_{10} [1 + \alpha \tau_{ij}]. \quad \text{Eq 9}$$

473 For comparing the combination and bi-specific therapies, we examined IIP and % viruses having IIP>2 (a
474 surrogate of protection in nonhuman primate studies¹⁷) for AUC and trough. Calculations were based on
475 500 simulations as implemented for the global sensitivity analysis.

476 **Realistic clinical trial simulation.** The full trial design contained a 12-week observation window and 600
477 mg total subcutaneous (SC) dosing with PK parameters established from clinical study (Table S1 and
478 **Supplementary Fig 4A**). To boost performance of 3BNC117 and 10-1074, we artificially enhanced their
479 half-lives by 3-fold to mimic an -LS variant (3BNC117-T and 10-1074-T). The distribution of *in vitro*
480 neutralization against circulating strains was modeled using *in vitro* derived IC50s from 507 available
481 common strains in the LANL CATNAP database²¹ (**Supplementary Fig 4B**).

482 We tested several models to map *in vivo* protection from *in vitro* neutralization. Pegu et al.
483 developed a logistic regression model to predict protection probability from *in vitro* neutralization titer¹⁷.
484 We use the output of their model at 50%, 75%, and 95% protection to test our model (**Supplementary Fig**
485 **4C**). Specifically, we employed the following approach: for a given bNAb (i) at a given concentration, we
486 estimated *in vivo* protection (p) using neutralization titer (τ_{ij}) against a virus (j). Using **Eq 3** and estimating
487 a single parameter, the potency reduction, found $\rho=1/91$ and led to reasonable fits. However, a better fit
488 was achieved using a 5-parameter logistic (5PL) model, a generalized dose-response type function with 5
489 parameters $\{A, B, C, D, E\}$ and the form
490

491 $y(x) = D + (A - D)\{1 + \exp[B(\log(x) - \log(C))]\}^{-E},$ Eq 10

492

493 here mapping *in vitro* titer $x = \tau_{ij}$ and to *in vivo* protection $y = p_{ij}$. We fixed $D = 0$ and $A = 1$ so that
494 protection ranges from 0-1. The remaining 3 parameters were estimated as $B = -1.84$, $C = 257$, and
495 $E = 0.338$. The best fit of the potency reduction model and the 5PL model are compared in

496 **Supplementary Fig 4C.**

497 We then illustrate predictions of the 5PL model for each bNAb via % viral coverage at *in vitro*
498 neutralization >50% compared to *in vivo* protection >50 and >95% in **Supplementary Fig 4D**. Using this
499 model of protection, we then calculated combined protection across the administered bNAbs (b is the
500 number of antibodies considered) assuming independence similar to Bliss-Hill:

501

502 $p_j = 1 - \prod_i^b (1 - p_{ij})$ Eq 11

503

504 We then defined our protection PKPD outcome as viral coverage fraction such that we can determine
505 what % of all viruses have protection above a certain threshold value X :

506

507 $f(t, X) = \frac{1}{n} \sum_{j=1}^n \mathcal{J}(p_j(t) > X)$ Eq 12

508

509 where \mathcal{J} is the indicator function equal to 1 if the inequality holds and 0 otherwise.

510 We assessed PKPD at the trough time (12-weeks, T) and as an average over the administration
511 period (AUC/T over time through T).

512

513 References

- 514 1 Stephenson KE, Wagh K, Korber B, Barouch DH. Vaccines and Broadly Neutralizing Antibodies for
515 HIV-1 Prevention. *Annu Rev Immunol* 2020;**38**:673–703. [https://doi.org/10.1146/annurev-](https://doi.org/10.1146/annurev-immunol-080219-023629)
516 [immunol-080219-023629](https://doi.org/10.1146/annurev-immunol-080219-023629).
- 517 2 Gao F, Bonsignori M, Liao HX, Kumar A, Xia SM, Lu X, *et al.* Cooperation of B cell lineages in
518 induction of HIV-1-broadly neutralizing antibodies. *Cell* 2014;**158**:481–91.
519 <https://doi.org/10.1016/j.cell.2014.06.022>.
- 520 3 Wang S, Mata-Fink J, Kriegsman B, Hanson M, Irvine DJ, Eisen HN, *et al.* Manipulating the Selection
521 Forces during Affinity Maturation to Generate Cross-Reactive HIV Antibodies. *Cell* 2015;**160**:785–
522 97. <https://doi.org/10.1016/j.cell.2015.01.027>.
- 523 4 Gilbert PB, Juraska M, DeCamp AC, Karuna S, Edupuganti S, Mgodhi N, *et al.* Basis and Statistical
524 Design of the Passive HIV-1 Antibody Mediated Prevention (AMP) Test-of-Concept Efficacy Trials.
525 *Stat Commun Infect Dis* 2017;**9**:. <https://doi.org/10.1515/scid-2016-0001>.
- 526 5 Corey L, Gilbert PB, Juraska M, Montefiori DC, Morris L, Karuna ST, *et al.* Two Randomized Trials of
527 Neutralizing Antibodies to Prevent HIV-1 Acquisition. *N Engl J Med* 2021;**384**:1003–14.
528 <https://doi.org/10.1056/NEJMoa2031738>.
- 529 6 Roychoudhury P, De Silva Felixge H, Reeves D, Mayer BT, Stone D, Schiffer JT, *et al.* Viral diversity
530 is an obligate consideration in CRISPR/Cas9 designs for targeting the HIV reservoir. *BMC Biol*
531 2018;**16**:75. <https://doi.org/10.1186/s12915-018-0544-1>.
- 532 7 Baeten JM, Donnell D, Ndase P, Mugo NR, Campbell JD, Wangisi J, *et al.* Antiretroviral Prophylaxis
533 for HIV Prevention in Heterosexual Men and Women. *N Engl J Med* 2012;**367**:399–410.
534 <https://doi.org/10.1056/NEJMoa1108524>.
- 535 8 Van Damme L, Corneli A, Ahmed K, Agot K, Lombaard J, Kapiga S, *et al.* Preexposure Prophylaxis
536 for HIV Infection among African Women. *N Engl J Med* 2012;**367**:411–22.

- 537 <https://doi.org/10.1056/NEJMoa1202614>.
- 538 9 Molina J-M, Capitant C, Spire B, Pialoux G, Cotte L, Charreau I, *et al*. On-Demand Preexposure
539 Prophylaxis in Men at High Risk for HIV-1 Infection. *N Engl J Med* 2015;**373**:2237–46.
540 <https://doi.org/10.1056/NEJMoa1506273>.
- 541 10 Kong R, Louder MK, Wagh K, Bailer RT, deCamp A, Greene K, *et al*. Improving Neutralization
542 Potency and Breadth by Combining Broadly Reactive HIV-1 Antibodies Targeting Major
543 Neutralization Epitopes. *J Virol* 2015;**89**:2659–71. <https://doi.org/10.1128/JVI.03136-14>.
- 544 11 Wagh K, Bhattacharya T, Williamson C, Robles A, Bayne M, Garrity J, *et al*. Optimal Combinations
545 of Broadly Neutralizing Antibodies for Prevention and Treatment of HIV-1 Clade C Infection. *PLoS*
546 *Pathog* 2016;**12**:e1005520-27. <https://doi.org/10.1371/journal.ppat.1005520>.
- 547 12 Schiffer JT, Swan DA, Magaret A, Corey L, Wald A, Ossig J, *et al*. Mathematical modeling of herpes
548 simplex virus-2 suppression with pritelivir predicts trial outcomes. *Sci Transl Med* 2016;**8**:324ra15-
549 324ra15. <https://doi.org/10.1126/scitranslmed.aad6654>.
- 550 13 Bournazos S, Gazumyan A, Seaman MS, Nussenzweig MC, Ravetch J V. Bispecific Anti-HIV-1
551 Antibodies with Enhanced Breadth and Potency. *Cell* 2016;**165**:1609–20.
552 <https://doi.org/10.1016/j.cell.2016.04.050>.
- 553 14 Wagh K, Seaman MS, Zingg M, Fitzsimons T, Barouch DH, Burton DR, *et al*. Potential of conventional
554 & bispecific broadly neutralizing antibodies for prevention of HIV-1 subtype A, C & D infections.
555 *PLoS Pathog* 2018;**14**:e1006860--24.
- 556 15 Gaudinski MR, Houser K V., Doria-Rose NA, Chen GL, Rothwell RSS, Berkowitz N, *et al*. Safety and
557 pharmacokinetics of broadly neutralising human monoclonal antibody VRC07-523LS in healthy
558 adults: a phase 1 dose-escalation clinical trial. *Lancet HIV* 2019;**6**:e667–79.
559 [https://doi.org/10.1016/S2352-3018\(19\)30181-X](https://doi.org/10.1016/S2352-3018(19)30181-X).
- 560 16 Scheid JF, Horwitz JA, Bar-On Y, Kreider EF, Lu C-L, Lorenzi JCC, *et al*. HIV-1 antibody 3BNC117
561 suppresses viral rebound in humans during treatment interruption. *Nature* 2016;**535**:556–60.
562 <https://doi.org/10.1038/nature18929>.
- 563 17 Pegu A, Borate B, Huang Y, Pauthner MG, Hessel AJ, Julg B, *et al*. A Meta-analysis of Passive
564 Immunization Studies Shows that Serum-Neutralizing Antibody Titer Associates with Protection
565 against SHIV Challenge. *Cell Host Microbe* 2019;**26**:336-346.e3.
566 <https://doi.org/10.1016/j.chom.2019.08.014>.
- 567 18 Reeves DB, Huang Y, Duke ER, Mayer BT, Fabian Cardozo-Ojeda E, Boshier FA, *et al*. Mathematical
568 modeling to reveal breakthrough mechanisms in the HIV Antibody Mediated Prevention (AMP)
569 trials. *PLoS Comput Biol* 2020;**16**:1–27. <https://doi.org/10.1371/journal.pcbi.1007626>.
- 570 19 Huang Y, Naidoo L, Zhang L, Carpp LN, Rudnicki E, Randhawa A, *et al*. Pharmacokinetics and
571 predicted neutralisation coverage of VRC01 in HIV-uninfected participants of the Antibody
572 Mediated Prevention (AMP) trials. *EBioMedicine* 2021;**64**:103203.
573 <https://doi.org/10.1016/j.ebiom.2020.103203>.
- 574 20 Huang Y, Zhang L, Eaton A, Mkhize NN, Carpp N, Rudnicki E, *et al*. Prediction of serum HIV-1
575 neutralization titers of VRC01 in HIV-uninfected Antibody Mediated Prevention (AMP) trial
576 participants Mediated Prevention (AMP) trial participants ABSTRACT. *Hum Vaccin Immunother*
577 2021;**00**:1–10. <https://doi.org/10.1080/21645515.2021.1908030>.
- 578 21 Yoon H, Macke J, West Jr AP, Foley B, Bjorkman PJ, Korber B, *et al*. CATNAP: a tool to compile,
579 analyze and tally neutralizing antibody panels. *Nucleic Acids Res* 2015;**43**:W213–9.
580 <https://doi.org/10.1093/nar/gkv404>.
- 581 22 Wagh K, Bhattacharya T, Williamson C, Robles A, Bayne M, Garrity J, *et al*. Optimal Combinations
582 of Broadly Neutralizing Antibodies for Prevention and Treatment of HIV-1 Clade C Infection. *PLoS*
583 *Pathog* 2016;**12**:1–27. <https://doi.org/10.1371/journal.ppat.1005520>.
- 584 23 Laskey SB, Siliciano RF. A mechanistic theory to explain the efficacy of antiretroviral therapy. *Nat*

- 585 *Rev Microbiol* 2014;**12**:772–80. <https://doi.org/10.1038/nrmicro3351>.
- 586 24 Einav T, Bloom JD. When two are better than one: Modeling the mechanisms of antibody mixtures.
587 *PLoS Comput Biol* 2020;**16**:1–17. <https://doi.org/10.1371/journal.pcbi.1007830>.
- 588 25 Hessel AJ, Jaworski JP, Epton E, Matsuda K, Pandey S, Kahl C, *et al*. Early short-term treatment
589 with neutralizing human monoclonal antibodies halts SHIV infection in infant macaques. *Nat Med*
590 2016;**22**:362–8. <https://doi.org/10.1038/nm.4063>.
- 591 26 Schiffer JT, Swan DA, Magaret A, Corey L, Wald A, Ossig J, *et al*. Mathematical modeling of herpes
592 simplex virus-2 suppression with pritelivir predicts trial outcomes. *Sci Transl Med* 2016;**8**:324ra15-
593 324ra15. <https://doi.org/10.1126/scitranslmed.aad6654>.
- 594 27 Lorenzi JCC, Mendoza P, Cohen YZ, Nogueira L, Lavine C, Sapiente J, *et al*. Neutralizing Activity of
595 Broadly Neutralizing anti-HIV-1 Antibodies against Primary African Isolates. *J Virol* 2020.
596 <https://doi.org/10.1128/jvi.01909-20>.
- 597 28 Mendoza P, Gruell H, Nogueira L, Pai JA, Butler AL, Millard K, *et al*. Combination therapy with anti-
598 HIV-1 antibodies maintains viral suppression. *Nature* 2018:1–21. <https://doi.org/10.1038/s41586-018-0531-2>.
- 600 29 Cale EM, Bai H, Bose M, Messina MA, Colby DJ, Sanders-Buell E, *et al*. Neutralizing antibody VRC01
601 failed to select for HIV-1 mutations upon viral rebound. *J Clin Invest* 2020;**130**:3299–304.
602 <https://doi.org/10.1172/JCI134395>.
- 603 30 Crowell TA, Colby DJ, Pinyakorn S, Sacdalan C, Pagliuzza A, Intasan J, *et al*. Safety and efficacy of
604 VRC01 broadly neutralising antibodies in adults with acutely treated HIV (RV397): a phase 2,
605 randomised, double-blind, placebo-controlled trial. *Lancet HIV* 2019;**3018**:1–10.
606 [https://doi.org/10.1016/S2352-3018\(19\)30053-0](https://doi.org/10.1016/S2352-3018(19)30053-0).
- 607 31 Wickham H, Averick M, Bryan J, Chang W, McGowan L, François R, *et al*. Welcome to the Tidyverse.
608 *J Open Source Softw* 2019;**4**:1686. <https://doi.org/10.21105/joss.01686>.
- 609 32 Davda JP, Dodds MG, Gibbs MA, Wisdom W, Gibbs JP. A model-based meta-analysis of monoclonal
610 antibody pharmacokinetics to guide optimal first-in-human study design. *MABs* 2014;**6**:1094–102.
611 <https://doi.org/10.4161/mabs.29095>.
- 612 33 Huang Y, Zhang L, Ledgerwood J, Grunenberg N, Bailer R, Isaacs A, *et al*. Population
613 pharmacokinetics analysis of VRC01, an HIV-1 broadly neutralizing monoclonal antibody, in healthy
614 adults. *MABs* 2017;**9**:792–800. <https://doi.org/10.1080/19420862.2017.1311435>.
- 615